CCSBT-OMMP/1706/04
(Agenda item 1)

OCEANS AND ATMOSPHERE
www.csiro.au

Updates required for new data sources and reconditioning of the CCSBT OM

Rich Hillary, Ann Preece, Campbell Davies

CCSBT-OMMP/1706/4
Prepared for the 8th Operating Model and Management Procedure Technical Meeting held in Seattle, U.S.A. 19th to the 23rd of June 2017

CSIRO
Oceans & Atmosphere
Castray Esplanade, Battery Point, Hobart TAS 7000, Australia
Telephone : +61 3 6232 5222
Fax : +61 3 6232 5000

Contents

Abstract

The CCSBT will be undertaking a stock assessment this year. The new MP development program will require both a reconditioning of the CCSBT OM and the inclusion - and future simulation - of new data sources. There are updates to longstanding OM data sets (catch composition, CPUE, aerial survey) as well as more parent-offpsring-pair close-kin data. There are also completely new data sources coming online now (the half-sibling pair close-kin data) and for next year (the first gene tagging data). In this paper we detail the changes made to the current suite of OM code (conditioning and projection) to accommodate and then simulate these new data sources. We also outline an initial reconditioning of the OM given the available data sources to assist in defining the relevant structure and settings of the OM for the presentation of the stock assessment at the coming ESC meeting.

1 Background

The current timetable for the immediate work program of the ESC is: (i) stock assessment this year, including new and updated data sources; (ii) development of methods for generating data to be used in the MP testing work starting in 2018; and (iii) adoption and implementation of a new MP in 2019 [1, 2]. This paper will cover the continuance of the first two work items - the stock assessment/reconditioning of the OM and data generation.

2 Material & Methods

This section is itself split into three main sections dealing with new and updated data sources, changes required to the conditioning code to accommodate these data, and finally changes required to the projection code to simulate them in the MP testing context.

2.1 Data: new and updated sources

2.1.1 Aerial survey

The last stock assessment in 2014 [3] contained survey data up to and including 2014. For this year we will have new data for 2016 and 2017, but none for 2015 given the survey was not undertaken that year. Figure 6.1 summarises the mean-standardised survey data up to and including 2017 data. As before, the 2014 survey was about twice the historical mean; the 2016 index was just over 4 times the historical mean; and 2017 was just under twice the historical mean.

Looking at the most recent years of Figure 6.1, while we do not have the 2015 data point, there is an apparent indication of sustained higher than average recruitment covering the 2011–2015 cohorts (assuming ages 2 to 4 in the survey data).

2.1.2 CPUE

The new data has been circulated in papers and via the information in the CPUE webinar in early June 2017.

2.1.3 POPs

The original POP data were generated using microsatellites, and contained information on the spawning abundance for 2002–2007 (because these are the cohorts of the juveniles in the original samples). The new POP data are generated using single nucleotide polymorphism (SNP) approaches, where we now have thousands of loci from across the genome. We do not propose to go into an in-depth report of the various pieces of detailed work that go into generating these data, merely a summary of what we found at a level relevant to the OM reconditioning work - see [4] for the details.

The new SNP-derived POP data does have some overlap with the previous data set, in terms of juvenile and adult coverage. Obviously, we genotyped all the previous POPs to ensure we could detect them

again this time around, and for adult capture year 2010 and juvenile cohorts 2002–2007 there was some overlap. To avoid potential double counting, we simply excluded data in the most recent SNP set that overlapped with the previous microsat data, thus making it simple to append the SNP data to the original data and include it in the updated OM without any additional changes being required.

For the updated SNP data (minus the overlap with the previous microsat data) we found 32 additional POPs, given 40,542,889 comparisons (previously we found 45 POPs given 38,180,182 comparisons). Overall, the simple empirical POP "index" (ratio of comparisons to POPs with summation across adult ages and capture years) is a little higher now than before, suggestive of slightly more optimistic signals, but is consistent in trend where there is cross-over with the previous POP data (see Figure 6.2). Given the complex role adult age-structure plays in the dynamics of POPs we do not infer anymore from the index summarised in Figure 6.2, and this is covered off in the detailed summary of the fits to the POP data later on. Table 2.1 summarises the number of comparisons at the juvenile cohort and adult capture year aggregation level, and Table 2.2 summarises the POPs at the same level.

	2006	2007	2008	2009	2010	2011	2012	2013	2014
2002	31	204	213	200	168	0	0	0	0
2003	275	1826	1912	1789	1504	1410	765	1387	1340
2004	361	2324	2381	2290	1971	1380	749	1358	1312
2005	300	1986	2071	1947	1640	1422	772	1399	1352
2006	0	1856	1944	1816	1530	1394	757	1372	1325
2007	0	0	2070	1939	1633	1387	758	1375	1328
2008	0	0	0	0	984	986	535	970	937
2009	0	0	0	0	952	954	518	939	907
2010	0	0	0	0	0	944	513	929	898
2011	0	0	0	0	0	0	512	928	897
2012	0	0	0	0	0	0	0	958	926

Table 2.1: *Number of juvenile-adult comparisons (in thousands) aggregated by juvenile cohort and adult year of capture.*

	2006	2007	2008	2009	2010	2011	2012	2013	2014
2002	0	0	0	0	0	0	0	0	0
2003	0	5	1	2	0	0	0	1	0
2004	0	2	0	0	3	0	0	0	0
2005	1	4	5	4	1	0	1	1	2
2006	0	4	3	2	0	0	0	0	0
2007	0	0	3	4	1	3	2	0	2
2008	0	0	0	0	0	1	1	1	0
2009	0	0	0	0	0	1	1	1	0
2010	0	0	0	0	0	3	1	4	0
2011	0	0	0	0	0	0	1	2	1
2012	0	0	0	0	0	0	0	1	1

Table 2.2: *Number of POPs aggreated by juvenile cohort and adult year of capture.*

2.1.4 HSPs

The detail on the HSP detection progress can be found in [4].

2.2 Changes to OM conditioning code

2.2.1 Population dynamics

The only change we suggest to the actual population dynamics is how we define the relative reproductive output-at-age for the population. Before the CKMR data it was basically a step function that was proportional to weight above age 10 and zero below it. We modified this for the original CKMR model, given obvious signs that there were clearly parents aged less than age 10, and where the apparent output of offspring was skewed more towards older/larger animals than weight-at-age suggested. The basic idea behind the original formulation of how we calculate the RRO-at-age will be the same. Now though, instead of being pre-calculated and included within the OM as a fixed vector, it will be calculated within the OM, take account of the changing distribution of of length-at-age over time, and have a control parameter included directly in the grid. The reasoning behind accounting for the changing length-at-age over time is because the fundamental assumption is that length is the primary driver of the reproductive dynamics, but age is the currency of the OM.

The core idea behind the drivers of the length-specific version (implicitly grouping sex), φ_l, are the same as before:

$$\varphi_l \propto w_l^{\psi} m_l,$$

where w_l and m_l are the length-specific weight and maturity relationships. The current model for m_l is a logistic relationship with $l_{50} = 150$ and $l_{95} = 180$ as previously used. The power parameter ψ is specifically there to permit cases where effective fecundity-at-length can be greater ($\psi > 1$) or less ($\psi < 1$) than proportional to weight - for example the notion of SSB would be $\psi = 1$. The current fixed value of $\psi \approx 1.72$ which was essentially chosen after looking at the predicted and observed POP adult age distribution, and was consistent with the stand-alone CKMR model in that the effective output of older/longer animals was far greater than a $\psi = 1$ model would have predicted. The reason for formally including it as a grid parameter is because, with the additional POP data over a long-time frame (we will have more POPs and more temporal coverage), we could - and arguably should - be estimating this key parameter. CKMR design work we have been doing here at CSIRO has demonstrated that you can, in principle, jointly estimate adult abundance, mortality and a parameter such as ψ fairly well with POPs, HSPs, and adult age data.

This defines the length-based setting for φ but we now need to translate this into an age-specific relationship for the OM. In the OM we have a time-dependent distribution of length-at-age, $\pi_{l|y,a}$, and following the idea that it is length that is the key driver for the reproductive dynamics, this implies we *should* be considering a time-varying setting for φ_a. This is calculated as follows:

$$\varphi_{y,a} \propto \int \varphi_l \times \pi_{l|y,a}, \mathrm{d}l. \tag{2.1}$$

so that we integrate over the year-specific distribution of length-at-age to get the expected value of RRO-at-age for that year. As before, everything is normalised by the maximum value for each year so that $\varphi_{y,a}$ is an ogive having values between 0 and 1. The spawning potential in each year is then effectively a weighted sum of spawning adults:

$$S_y = \sum_a N_{y,a} \varphi_{y,a}.$$

To bring the ψ parameter into the grid is, we feel, a sensible first step to trying to estimate the parameter. It may be possible in later assessments to treat ψ as a fully free parameter (like M_4 or M_{30}), but it perhaps make sense to start with a grid approach for now (so we can use prior vs. likelihood weighting initially to explore information content). We propose an initial grid vector of three values: $\psi^{\mathrm{grid}} = \{1.5, 1.75, 2\}$. Figure 6.3 shows the three associated vectors ϕ_a (including the current vector) for the most recent distribution of length-at-age, encompassing the CK data in the OM.

The range of values for φ_a is not large - for a total mortality $Z = 0.2$ the range in per-recruit spawning potential is about 20–25%. As with all grid elements, we can look at prior and likelihood weighting,

and augmenting or fundamentally changing the range as required. We just felt that this initial range encapsulated the historical values, while allowing for some uncertainty therein and a chance to explore information content in a stable fashion at first.

2.2.2 Revised grid configuration

At the moment we have a 6-d grid: $\boldsymbol{\theta}^g = \{h, M_0, M_{10}, \omega, I^{\text{cpue}}, a^{\text{cpue}}\}$ with dimensions 5 x 4 x 4 x 1 x 2 x 2 = 320 unique combinations. Augmenting the grid $\boldsymbol{\theta}^g = \{h, M_0, M_{10}, \omega, I^{\text{cpue}}, a^{\text{cpue}}, \psi\}$ and with 3 possible values for ψ would be a grid of size 960 (which is a lot). We propose a coarsening of the grid for steepness and M_{10} to ameliorate this augmentation to the grid:

- For steepness, instead of $h = \{0.55, 0.64, 0.73, 0.82, 0.9\}$, we propose $h = \{0.55, 0.67, 0.78, 0.9\}$ so a reduction from 5 to 4 elements
- For M_{10}, instead of $M_{10} = \{0.05, 0.075, 0.1, 0.125\}$, we propose $M_{10} = \{0.05, 0.085, 0.12\}$ so a reduction from 4 to 3 elements

This would give us 576 grid combinations, versus 320 as before but far less than the full 960 if we just added ψ into the grid and changed nothing else. We only sample from a uniform prior for steepness at the moment, so if we maintain the range (as above) but simply have one less element in the grid, we obtain the variation in resilience we had before without any obvious information loss or bias. For M_{10}, the most sampled values are the lower values, 0.05 and 0.075, with a much lesser weight being assigned by the OM to 0.1 and 0.125 at the moment. We feel we can sensibly reduce the number of options by 1 grid element, while again maintaining the sampled range. Any impacts of these changes can be evaluated in the proposed staged reconditioning of the OM, relative to the 2014 reference set and associated robustness tests.

2.2.3 HSP likelihood

In the two main OMMP papers on OM changes [5] and data generation [6] from last year we outlined what the HSP probability (when comparing juveniles belonging to different cohorts) would look like. It's worth restating that general probability here, and then outlining some of the modifications and accommodations we are likely to need to make in the OM log-likelihood to deal with the real world data.

For a number of reasons (highly variable larval survival of siblings, confusing N with effective breeding population N_b) we avoid doing within-cohort comparisons. When comparing juveniles i and j - belonging to cohort c_i and c_j, respectively - we only consider $c_i \neq c_j$. The probability of these two juveniles being HSPs (sharing a mother *or* a father) is:

$$p^{\text{hsp}} = \frac{4q^{\text{hsp}}}{S_{c_{\max}}} \left(\sum_a \left[\gamma_{c_{\min},a} \exp\left(- \sum_{y=c_{\min}}^{c_{\max}-1} Z_{y,a+y-c_{\min}} \right) \varphi_{y+\delta,a+\delta} \right] \right), \tag{2.2}$$

$$\gamma_{y,a} = \frac{N_{y,a}\varphi_{y,a}}{S_y}, \tag{2.3}$$

$$\delta = |c_i - c_j|, \tag{2.4}$$

$$c_{\min} = \min\{c_i, c_j\}, \tag{2.5}$$

$$c_{\max} = \max\{c_i, c_j\}. \tag{2.6}$$

In terms of an explanation of the various pieces of the HSP probability: we don't see the adult in this scenario, so we must integrate over all possible adult ages $\gamma_{c_{\min},a}$ in the earliest cohort; we then account for the probability that an adult survives to the birth of the second, younger fish at time $c_{\max}$ (terms involving Z); we then, accounting for any additional increases in relative fecundity over that period between birth years, calculate the relative reproductive output of the adult at the time of birth of the later cohort ($\varphi_{y+\delta,a+\delta}$ and the term in $S^{-1}_{c_{\max}}$ at the front). The factor of 4 comes from the following implication of

assuming a 50/50 sex ratio: If $N_{♂} = N_{♀} = N/2$, then for the within-cohort case (even though we avoid it, but that doesn't affect the argument) then the probability of being either a maternal (share a mother) or paternal (share a father) HSP is $p^{\text{hsp}} = 1/N_{♂} + 1/N_{♀} = 2/N + 2/N = 4/N$. So, the factor of 4 just comes from implicitly assuming a 50/50 sex ratio in the OM. If either the updated POPs *and/or* the HSP mtDNA data suggest this is not likely to be a reasonable assumption, we may need a pseudo-sex specific model to accommodate that, but we won't know that until we fit the models and look at the mtDNA results and see whether they are compatible with an approximately 50/50 sex ratio.

In an ideal situation, the HSP probability would define the Bernoulli likelihood in the OM for each individual comparison between juveniles i and j. The probability is the same for all such comparisons where the two key covariates, c_i and c_j are the same, so we can group these comparisons together into a binomial likelihood with probability p^{hsp} and sample size $n_{c,c'}$, which is just the total number of juvenile comparisons done between fish from cohorts c and c'. This would be feasible **if** we could cleanly identify **every** single HSP without there being any chance of false positive contamination from genuinely unrelated pairs or other types of kin (primarily half first-cousins or half auntie/uncles).

The original microsat approach to finding POPs used Mendelian exclusion - true POPs should share at least one allele at all locations. This resulted in a set of clear POPs (with a false positive rate of less than 1 POP) for that particular data set. With HSPs and SNPs (as opposed to microsats) the issue is a bit more complex. In the genetic inheritance sense, at any given locus we either share 0, 1 or 2 alleles that are identical by descent (IBD). A unique weight vector $\mathbf{k} = \{k_0, k_1, k_2\}$, which sums to 1, determines the chance that two individuals share alleles that are IBD at a given locus for all the different kin types (unrelated, parent-offspring, half-sibling etc.). For two unrelated individuals (UP) $\mathbf{k}_{\text{up}} = \{1, 0, 0\}$; for a POP $\mathbf{k}_{\text{pop}} = \{0, 1, 0\}$; for a full-sibling pair (FSP) $\mathbf{k}_{\text{fsp}} = \{0.25, 0.5, 0.25\}$; and for an HSP $\mathbf{k}_{\text{hsp}} = \{0.5, 0.5, 0\}$.

Using this information, we can construct a likelihood based statistic that can help us find if a specific comparison pair of individuals is actually of a specific kin type (e.g. HSP), relative to them being assumed to be unrelated (i.e. an UP). Specifically, we construct something called a pseudo log-odds ratio (hereafter PLOD) summed across all loci for a given comparison kin test (UP *vs.* HSP) between fish i and fish j: PLOD(i, j | HSP). This all sounds a bit esoteric at this point so we've included an example with a small data set. With SBT there are millions of comparisons and any summary plot would both be too big and impossible to see. However, for a PLOD summary plot (Figure 6.4) looking for HSPs in a sample of 116 juvenile river sharks (*Glyphis glyphis*) from a river in Northern Australia, the principle is much clearer to see we think. For n samples, there are $n(n-1)/2$ unique cross-comparisons so here we have 6,670 in total.

Looking at Figure 6.4 you see the vast majority of samples are distributed around the blue dotted line in the lower half of the figure. This is where the allele frequency model and the $\mathbf{k}_{\text{up}}$ IBD model expects unrelated pairs' (UPs) PLODs to be, and that is where they appear. In the upper half of the figure we see the dotted magenta line which is were we would expect the HSP PLOD to be. If we had more loci (there are 1,500 used here as with the SBT SNPs this time around) there would be no overlap between the UPs and less related animals (cousins and uncles/aunties) at the bottom of the figure, and the true HSPs in the top of the figure. The threshold value of the PLOD at which we would not expect to see any true UPs is around -0.004. So, anything appearing above this line would be expected to be an related (in some way) pair - the three closest candidates being half cousins (HCPs who share a grandparent), half auntie/uncles (half-thiatic pairs or HTPs), or HSPs (and no more if all the repeat fish and FSPs have been removed). Look above this UP false-positive threshold level though and we see a disperse but continuous cloud of comparisons until we hit the likely true HSPs levels at the top of the plot. What we want is a threshold value of the PLOD statistic, call it η, such that we would expect to find effectively zero non-HSP kin (HCPs, HTPs) above this level - i.e. only HSPs. The cut-off for HCPs is just below the zero line; for HTPs (the most extreme cut-off) is around 0.008. So, in terms of the data we actually will use, we take

the comparisons above this cut-off of $PLOD > \eta \approx 0.008$ and discard any below this.

This is us actively controlling the false positive rate so that we have effectively less than 1 non-HSP appearing in the HSP data. The usual drawback in these cases is that you can control for false-positive rates, but you have to live with the resultant false-negative rate - this will definitely not be zero unless you are very lucky. We will discard some true proportion of the total set of HSPs and that needs to be reflected in the likelihood. What we need in the likelihood calculations later is the following: $\mathbb{P}\left(PLOD_{i,j} \leq \eta \,|\, HSP\right)$. This is the proportion of **true** HSPs we expect to lose by having to set η high enough so that we have effectively zero non-HSPs appearing in the pairs with PLODs above this threshold level. We calculate this probability in a two-step way:

1. Using the comparisons that appear above the magenta line ($\mathbb{E}(PLOD \,|\, HSP)$), compute the 1-sided variance as an estimate of the true variance $\mathbb{V}(PLOD \,|\, HSP)$ (which we can't predict theoretically, unlike for the UP case)
2. Assuming a normal distribution for the HSP PLOD statistic, calculate the probability of a true HSP PLOD being below η: $\mathbb{P}\left(PLOD_{i,j} \leq \eta \,|\, HSP\right)$

The quantity we need in the log-likelihood is $\pi_\eta = 1 - \mathbb{P}\left(PLOD_{i,j} \leq \eta | HSP\right)$ - i.e. the proportion of true HSP values found above a PLOD threshold of η. For each $\{i, j\}$ comparison group, we then modify the base probability in the binomial likelihood as follows:

$$\ell\left(k_{i,j} = HSP \,|\, \eta, \mathbf{z}, \cdots\right) \propto \left(\pi_\eta p_{i,j}^{\mathrm{hsp}}\right)^{K_{i,j}} \left(1 - \pi_\eta p_{i,j}^{\mathrm{hsp}}\right)^{n_{i,j} - K_{i,j}}, \tag{2.7}$$

where $K_{i,j}$ is the number of comparisons with a PLOD above the cut-off η, and $n_{i,j}$ the total number of comparisons for the given covariates $\mathbf{z} = \{c_i, c_j\}$. So, what we are really modelling is not the HSP probability, but the probability of having a particular comparison's PLOD above the cut-off η. As with the POP likelihood, we have assumed a Bernoulli base likelihood, which forms into a binomial given the comparison grouping. This would be easy to extend to being a beta-binomial likelihood if required and we don't detail the algebra here.

There are a few select ways that could bias the information in the HSP data, with respect to absolute abundance. The first is non-HSP kin contaminating the sample, and we've outlined how to take care of that in the previous section. We calculate the relevant PLOD cut-off, η, and use only comparisons with a PLOD above this level. The resultant false-negative loss-rate is also factored into the likelihood. There will, however, given the empirical nature of the estimate of $\mathbb{V}(PLOD \,|\, HSP)$ and the choices required to choose the cut-off value, η, be some uncertainty in this estimate. This will get taken up in the estimate of q^{hsp}

Another plausible factor would be unexpected spawning-related juvenile dynamics. Specifically, we do not mean just the alternative juvenile disperal hypotheses we explore in the gene tagging design work [7]. We mean a more complex situation where there are specific adults who spawn at a specific site/time, whose offspring recruit to say the GAB, and another subset of distinct set of adults who spawn at alternative sites/times whose offspring recruit to somewhere other than the GAB, and *never* spend time in the GAB as a juvenile. In this scenario, what we are really doing by sampling only the GAB-recruiting animals is effectively measuring the size and demography of the adults whose juveniles recruit to the GAB. For the POP data, we will still have something potentially strange going on by only looking at GAB juveniles *but* we would have covered all the spawning adults when doing so, and any bias would be different to the HSP case (where we are potentially indirectly looking only at a subset of spawning adults). Such an issue could be explored by sampling juveniles that were demonstrably *not* in the GAB during summer.

The one effect that we can probably say is likely to be true with the information we have now, and one where we can actively explore the level and direction of the bias, is individual variation in reproductive success. In this document, we assume length to be the key driver of reproductive success - itself a proxy

for weight really and keep this in mind for later. In the OM we integrate over the population distribution of length-at-age to get the expected age-specific relative reproductive output $\varphi_{y,a}$. However, if we assume (as contemporary growth models often do) that each animal has a specific length-at-age relationship, we are introducing a bias into the HSP probability. It's not a bias in the POP probability, but a source of over-dispersion. However, for HSPs we account for relative reproductive output *twice*: once at the birth of the older fish, and again at the birth of the younger fish. This bias effect is something akin to 'unmodelled heterogeneity in the probability of recapture' in mark-recapture models. Individual variation in RRO compounds here (sort-of-quadratically) in a way that it does not for the POP case. Using a basically identical life-history we simulated what effect this might have for SBT:

- Simulate HSP data with a resultant detection rate (i.e. number of comparisons to abundance ratio) the same as the current sampling program for SBT
- For one case, assume the population-level relationship for $\varphi_{y,a}$; for the other case sample a specific vector of $\varphi_{y,a}$ for each putative adult in the simulated comparisons (given φ_l and $\pi_{l|y,a}$)
- For both cases, back-estimate adult abundance and mortality

Our initial explorations suggest that, as we would expect, adult mortality is unbiased by this effect if it is not strongly dependent on length, but it can be dependent on age (senescence). There is a small positive bias in the estimates of adult abundance (not more than 5%), so we might be weakly over-estimating adult abundance if we ignore the effect. One major caveat is that this is the extreme case we consider here: we assume length as a proxy for weight and that this dominates the RRO relationship-at-age. When actually looking at the weight-at-length data in the adults, we actually see a weak *negative* correlation between observed length and individual values of the b parameter in the $w_l = al^b$ relationship. This suggests that, at least for SBT, there is some indication that lifetime shorter/longer animals are fatter/thinner in a relative sense (i.e. their 'condition' parameter b), which would - if weight is really the fecundity controller - act to ameliorate this effect in the HSP data.

For now, we recommend keeping q^{hsp} as a fully estimable parameter in the first exploratory round of including the HSP and the POP data together. If $q^{\mathrm{hsp}} \approx 1$ and at levels we saw for the simulation testing, we feel we have some idea what might be causing it to differ from 1. If it is - for whatever reason - significantly different from 1 then we need to discuss why this might be the case. Having it as a fully estimable parameter will obviously reduce the HSP information content with respect to absolute adult abundance, but **not** on trend and adult mortality. We have the POP data for absolute abundance and relative reproductive output, so this might be a conservative but sensible route at this stage - in terms of actively estimating q^{hsp} in this round of work.

2.2.4 Gene-tagging likelihood

The nature of the gene tagging estimator (modified Petersen-type estimate) as well as the proposed likelihood structure (beta-binomal with over-dispersion an - eventually - tuned control parameter) have already been detailed in [5].

2.3 Changes to OM projection code

There are only minor changes required to the population dynamics code in the projection module to accommodate the new definition of RRO-at-age, $\varphi_{y,a}$. We make the usual assumption that the most recent values continue to be used into the future (as future growth and selectivity are currently defined). Major changes will, however, be required to simulate the GT and the POP and HSP data. Each data source is sample-size driven, which is itself a control variable that the CCSBT and its member scientists have differing degrees of influence over.

For the GT program, we have target levels of initial releases and follow-up catch sampling numbers the following year. The initial release numbers will be somewhat variable, given this is a highly dynamic

sampling arena (the GAB), and something we are going to improve at over time. For example, in 2016 we tagged almost 4,000 fish; in 2017 we tagged over 7,500 fish. The catch sampling part of the program is a more controllable process, and likely something we can expect to be less variable than the release side of the field operations. One of the primary motivations of the initial sample size numbers is to attain a general total level of samples in the 15,000 range, so the catch sampling can be modified if a short-fall in releases occurs, and we can "double-dip" the HSP CKMR juvenile samples at the catch sampling end of things if required. At the OMMP we can discuss a sensible set of scenarios from which to define simulation protocols for the GT sample sizes that cover off on this type of inherent variabiliy - and associated catch sampling modifications - we are going to observe. In terms of simulating the data for a given sampling regime, we will use the likelihood function but also consider some additional robustness trials exploring potential bias scenarios [7].

For the close-kin sampling programs, these are more controlable than the GT case. The program samples M_i adults and M_j juveniles (within the age 3 length range) in Indonesia and Port Lincoln, respectively. The initial POP data compared adults and juveniles *only*, and the initial HSP data set will be juvenile-juvenile comparisons for now. Once these data are fitted within the model, we have a functional likelihood for both from which to simulate the data. We can also explore adpative schemes for both the adult and juvenile sampling schemes to see what difference these make both in terms of overall POPs and HSPs found in the future, and the effect this might have on an MP using these data. One consideration, in this respect, is whether it would be sensible to explore the sample sizes required to have a reasonable expectation of a minimum number of POPs and HSPs for each cohort covered in the samples.

3 Results

We have broken down the results section in three main subsections:

1. How to get from where the OM results placed us in 2014 to the present, when we have a variety of new and updated data and structural changes planned for both the OM population dynamics model and the grid
2. Preliminary results and fits to the data for the putative reference set of OMs
3. Implications arising for data generation and the MP testing process for 2018

3.1 Preliminary results arising from reconditioning the OM

The suggested updated grid structure we used for the OM results presented in this subsection is summarised in Table 3.1. This is actually a modified grid, relative to the one suggested in Section 2.2.2 due to the fact that a large proportion of runs with $h = 0.55$ crashed on initial model explorations. This is presumably being driven by: more POP data and an overall slightly more optimistic outlook from these data; the two new aerial survey data points that suggest recent recruitment is well above the average; and recent CPUE data now at levels seen in the 1980s. The grid combinations with the lowest steepness are almost always the most pessimistic in terms of stock status and recent trends therein, so it is not that surprising that these values are generally incompatible with the updated data.

The final number of grid combinations is now 432 (versus 320 in 2014) and, in combination with the updated data and OM changes, takes a little longer to run a full set than before, though not significantly (something like 3.5–4 hours on a recent laptop with decent specifications).

Figure 6.5 shows the absolute spawner abundance and spawner depletion summaries (median and 80% PI) for the **base2016sqrt** grid and data configuration and Figure 6.6 shows the recruitment summary.

All fits presented are for the best-fitting grid cell. The fits to the relative abundance indices (long-line CPUE and the aerial survey) are summarised in Figure 6.7. The fits to the tagging data (aggregated to the cohort-of-release and recapture-age level) are summarised in Figure 6.8. Figure 6.9 summarises the

Parameter	Values	CumulN	Prior	Sampling
h	0.65, 0.78, 0.9	3	uniform	Prior
M_0	0.35, 0.4, 0.45, 0.5	12	uniform	ObjFn
M_{10}	0.05, 0.085, 0.12	36	uniform	ObjFn
ω	1	36	uniform	Prior
CPUE	w0.5, w0.8	72	uniform	Prior
CPUE ages	4–18, 8–12	144	0.67, 0.33	Prior
ψ	1.5, 1.75. 2	432	0.25, 0.5, 0.25	Prior

Table 3.1: *New suggested grid structure for the OM.*

fits to the updated POP CKMR data at two aggregation levels: (i) the juvenile cohort level (aggregated across adult capture year and age); and (ii) the adult capture age level (aggregated across adult capture year and juvenile cohort). The juvenile cohort aggregation level will show if we are systematically over or under-estimating overall adult abundance. The adult capture age aggregation level will show whether we are getting the adult age structure in the POPs about right and, hence, the RRO-at-age model ($\varphi_{y,a}$) is adequate. Figure 6.10 details the fits to the age data sets (Indonesian and surface fisheries). Figure 6.11 details the fits to the length data sets (fisheries LL_{1-4}).

Fits to the long-line CPUE data are good (Figure 6.7), with the observed data -barring the historical minimum in 2007 - falling within the predicted 95% range. Fits the aerial survey data (Figure 6.7) are similar to before, with some of the lower points and the historical high of 2016 sitting outside the predicted 95%ile, but the overall trend fitted fine. The fits to the tagging data (Figure 6.8) are good and qualitatively unchanged from previous years - some minor tension between the 1994 and 1995 release cohorts, but the major recapture cohorts (1996 and 1997) are fitted well. The updated POP data are fitted well (Figure 6.9) at both the juvenile cohort and the adult capture age aggregation levels. This suggests that we are not over or under-estimating current spawning abundance as informed by the POP data. It also suggests we are getting the adult age structure in the POPs correct, and we can have some faith in the $\varphi_{y,a}$ parameters in defining the age-structure of the relative reproductive out (RRO). Fits to the fisheries with age data (Indonesian and surface) are generally good (Figure 6.10). Fits to the fisheries with length data (long-line fisheries LL_{1-4}) are similar to previous years. Fits to LL_1 and LL_2 are fine for most year, but for LL_3 and LL_4 - as before - there are years of clear misfit. These are linked to years with little to no sampling coverage (and which receive) no weight in the OM conditioning, and need adjusting to remove years with zero effective sample size.

3.2 Bridging analysis from 2014 to present

There are a number of routes that we could take to move from the 2014 OM to the present, given new and updated data sources as well as structural changes to the OM this time around. There are updated data sources (catch composition, CPUE, survey data) as well as what could be considered both new data and updated data (SNP derived POP data) and we think it sensible to consider splitting these for the moment, at least in terms of a bridging path from 2014 to the present. The structural changes to the OM are both in terms of population dynamics (the time-varying age-specific reproductive output parameter $\varphi_{y,a}$) and the grid (addition of a new parameter, ψ, as well as modifications to the ranges and values of the other grid elements).

The one major data-specific change (beyond updates of CPUE, aerial survey and catch composition) is new inclusion of the SNP derived POP data, alongside the microsat POP data from previous years. Figure 6.12 shows the absolute SSB and depletion relative to the unfished state for both all years and from 1985 to the present, with and without the new CKMR POP data. They are both very consistent, with the OM using all the POP data with a slightly higher spawner abundance than before (as we expected given the comparison-to-POP ration generally being a little higher now). Depletion levels are more similar,

though again with the OM using all the data slightly higher than the one using only the microsat POP data. This suggests that the revised POP data are very consistent with the previous data where they overlap, and that the projected recent increase in spawner abundance we saw in 2014 is actually validated with the new POP data (as they cover the period 2002–2012, not 2002–2007 as before).

3.3 Implications for data generation in MP testing

We have no current GT data in the model, so we cannot update any thoughts on the data generation model for these data. For the CPUE we see no obvious recent levels of misfit, though we are to explore the catchability change scenarios post-2008 for the MP work. For the POP CKMR data, the fits look good - though we have not yet done any full predictive analyses as in previous years to assess potential levels of over-dispersion in these data. Initial considerations suggest - as before - there is no clear over-dispersion in these data and that our current likelihood configuration will suffice for data generation purposes. We have no HSP CKMR data included in the OM as yet so we cannot comment on issues relating to these data and generation for MP testing.

4 Discussion

For the initial updated OM (in terms of both structure, grid options and updated data) we have been able to fit to all the updated data (in terms of indices of abundance, catch composition, and the CKMR POP data). Fits to the indices of abundance (CPUE, aerial survey) are similar to previous years. Fits to the 1990s tagging data are good and remain similar to previous OM reconditioning results. The fits to the updated CKMR POP data are good, suggesting we are getting the overall level of recent spawner abundance right as predicted by these data, and the age structure in the POPs also. This gives us some confidence not just in our recent spawner abundance estimates, but also in the revised form of the relative reproductive output model as defined by $\varphi_{y,a}$. The fits to the catch composition (both age and length) are fine and similar to previous years. In terms of spawning depletion, current levels (*ca.* 2017) are estimated to be 0.14 (0.11–0.18) in terms of median (and 80% PI) for the putative reference set. Recent recruitment (especially 2013) were estimated to be well above the expected level predicted by the stock-recruit relationship, driven by the high survey points in 2014, 2016 and 2017 and the increasing level of recent mean long-line CPUE also.

A factor we have not explored in this paper, or in the current OM runs, is finding kin (both POP and HSP and others) when comparing adults and adults in the POP and HSP sense, or juveniles and adults in the HSP context. As the CK data sets become larger, these comparisons are likely to begin to yield a number of matches that could become informative (i.e. not just abundance but M_{10}, RRO, senescence and so on). For example, take two adults that are found to be a POP (and we can sensibly discern which is the offspring and which is the parent). This contains information on adult abundance in the birth year of the offspring, which might be further back in time than the previous offspring found in the juvenile-focussed POPs and therefore extends the information range of the data back beyond the current boundary of 2002 (the earliest juvenile cohort in the data). Another case is finding what we think is an HSP in an adult-adult comparison - this contains information on the period between the two birth years of the adults and, as before, could extend the information range historically. We might have to factor in the chance of this being a grandparent-grandoffspring pair (GGP) as these are indistinguishable from HSPs, genetically speaking. The main point is that, once we have both data sets in the OM and fitting together, we can consider a wider array of comparisons to that could increase both the information content and historical range of the CK data overall.

5 Acknowledgements

This work was funded by the Australian Fisheries Management Authority, and CSIRO Oceans & Atmosphere. Mark Bravington & Paige Eveson are thanked for all their work on the SNP design and kin finding pipeline.

References

[1] Report of the 21st Meeting of the Scientific Committee. CCSBT, Kaoihsiung, Taiwan, September 2016.

[2] Report of the 23rd Annual Meeting of the Commission. CCSBT, Kaoihsiung, Taiwan, October 2016.

[3] Hillary, R. M., Preece, A., and Davies, C. R. (2014) Assessment of stock status of southern bluefin tuna in 2014 with reconditioned operating model. *CCSBT-ESC/1409/21*.

[4] Bravington, M. V. *et al.*. (2017) Update on new POP and HSP data for 2017 ESC work.

[5] Hillary, R. M., Preece, A., and Davies, C. R. (2016) Reconsideration of OM structure and new data sources for 2017 reconditioning. *CCSBT-OMMP/1609/4*.

[6] Hillary, R. M., Preece, A., and Davies, C. R. (2016) Methods for data generation in projections. *CCSBT-OMMP/1609/7*.

[7] Preece, A., Eveson, J. P., Davies, C. R., Grewe, P. G., Hillary, R. M., and Bravington, M .V. (2015) Report on gene-tagging design study. *CCSBT-ESC/1509/18*.

[8] Bravington, M. V., Skaug, H. J., and Anderson, E. C. (2016) Close-kin mark-recapture. *Stat. Sci.* **31**: 259–275.

6 Figures

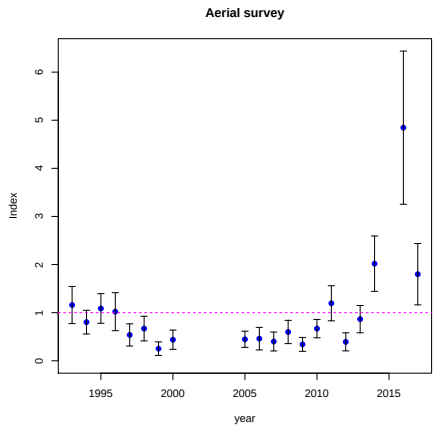

Figure 6.1: *Summary (in terms of point estimates and approximate 95% CI) of the mean-standardised aerial survey for data up to and including 2017.*

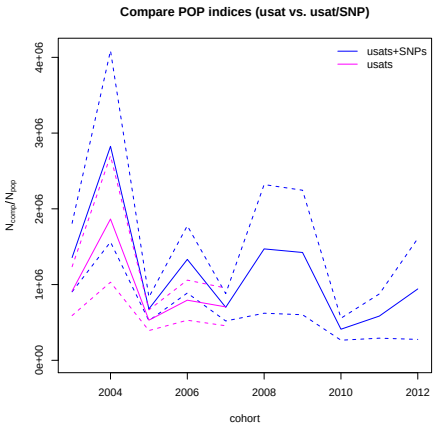

Figure 6.2: *Simple, empirical POP "index" summary (ratio of comparisons to POPs for the relevant juvenile cohort, summed across adult capture years and ages). The full line is the actual index with the dotted lines an approximate ± 1 s.e. using the inverse number of POPs to calculate a CV (square-root thereof).*

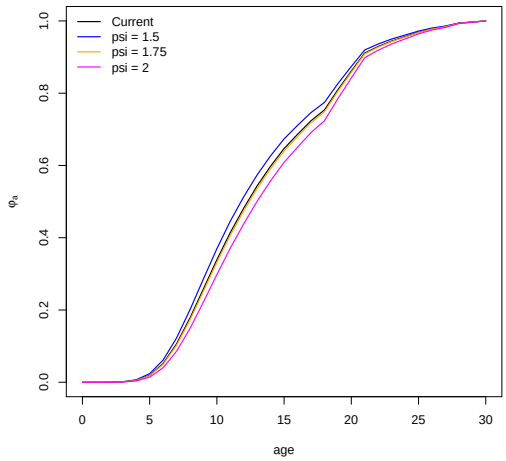

Figure 6.3: *For the most recent distribution of length-at-age, covering the CK data in the OM, the three associated φ_a vectors given the proposed grid values of ψ, and the one currently used in the OM.*

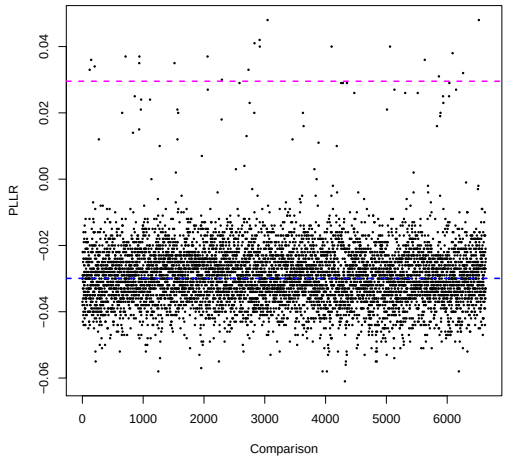

Figure 6.4: *PLOD (PLLR) for 6,670 comparisons of 116 fish when asking whether they are UPs (in the bottom around the dotted blue line) or HSPs (in the top half around the dotted magenta line).*

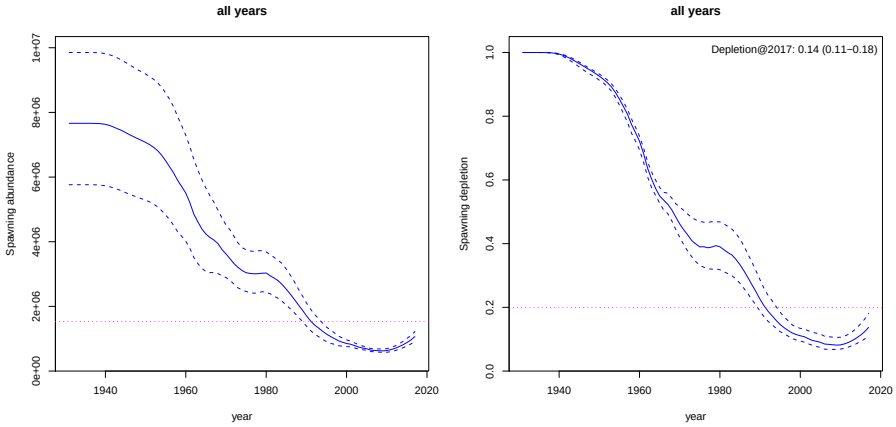

Figure 6.5: *Median (full line) and 80% PI (dotted line) for absolute spawner abundance (left) and the relative depletion thereof (right) - the final year is 2017, the first 1931. The magenta dotted line is 20% of the unfished level (ca. 1931).*

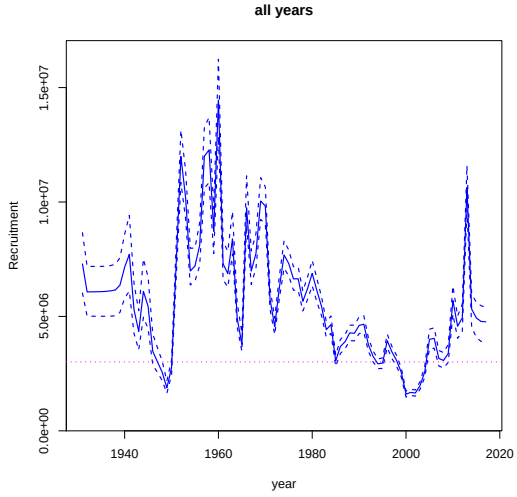

Figure 6.6: *Median (full line) and 80% PI (dotted line) for recruitment - the final year is 2017, the first 1931. The magenta dotted line is 50% of the unfished level (ca. 1931).*

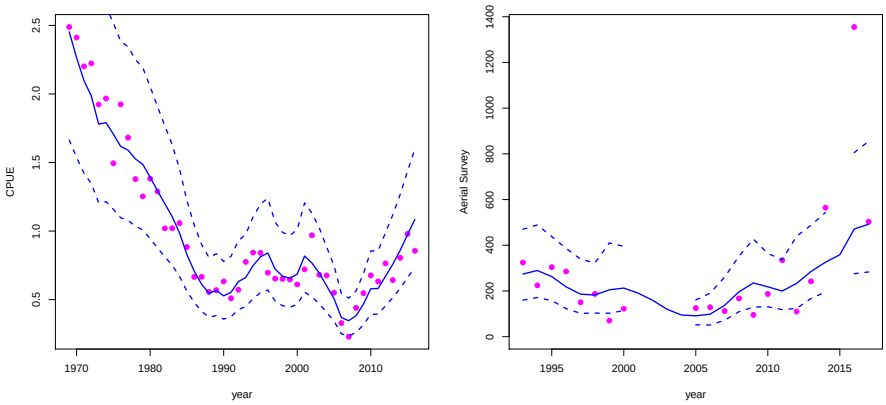

Figure 6.7: *Fits (for the best-fitting grid cell) to the long-line CPUE (left) and aerial survey (right) indices. Magenta dots are the observed data and the model-predicted expected (full blue line) and approximate 95% CI (dotted blue line) index.*

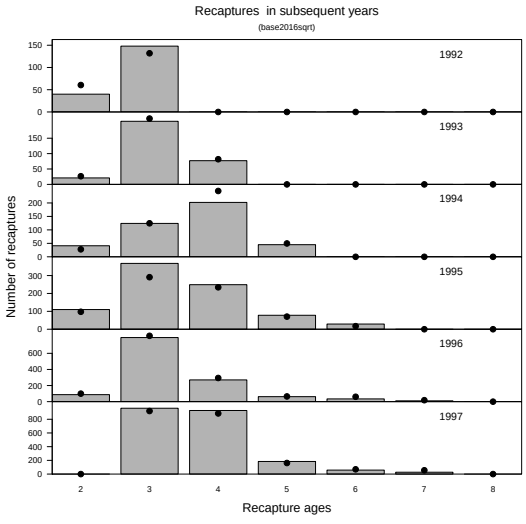

Figure 6.8: *Fits to the tagging data, aggregated to the cohort-of-release and recapture-age level, for the best-fitting grid cell.*

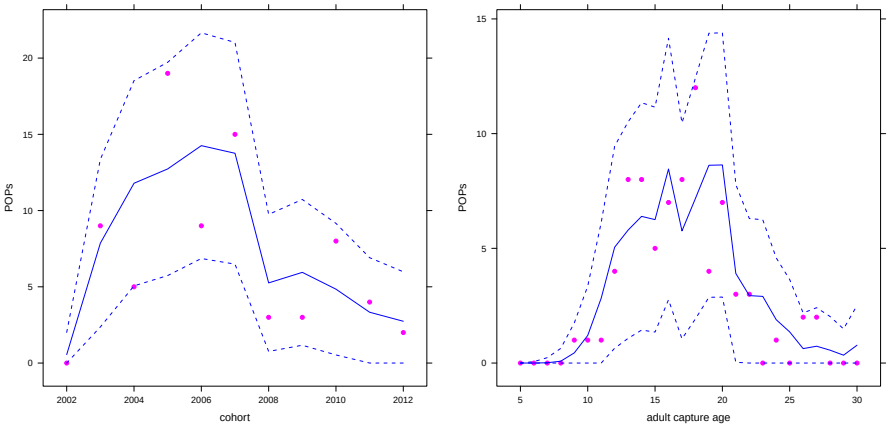

Figure 6.9: *Fits (for the best-fitting grid cell) to the updated POP CKMR data. Magenta circles are the observed data with the model predicted expected value (full blue line) and approximate 95% CI (dotted blue line). On the left the data are aggregated to the juvenile cohort level (across adult capture year and age). On the right the data are aggregated to the adult capture age level (across adult capture year and juvenile cohort).*

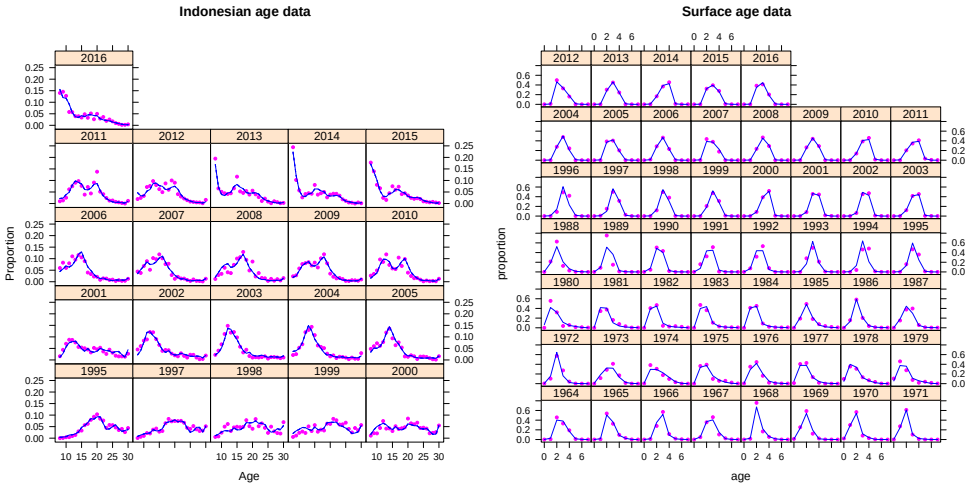

Figure 6.10: *Fits (for the best-fitting grid cell) to the age data for the Indonesian (left) and surface (right) fisheries.*

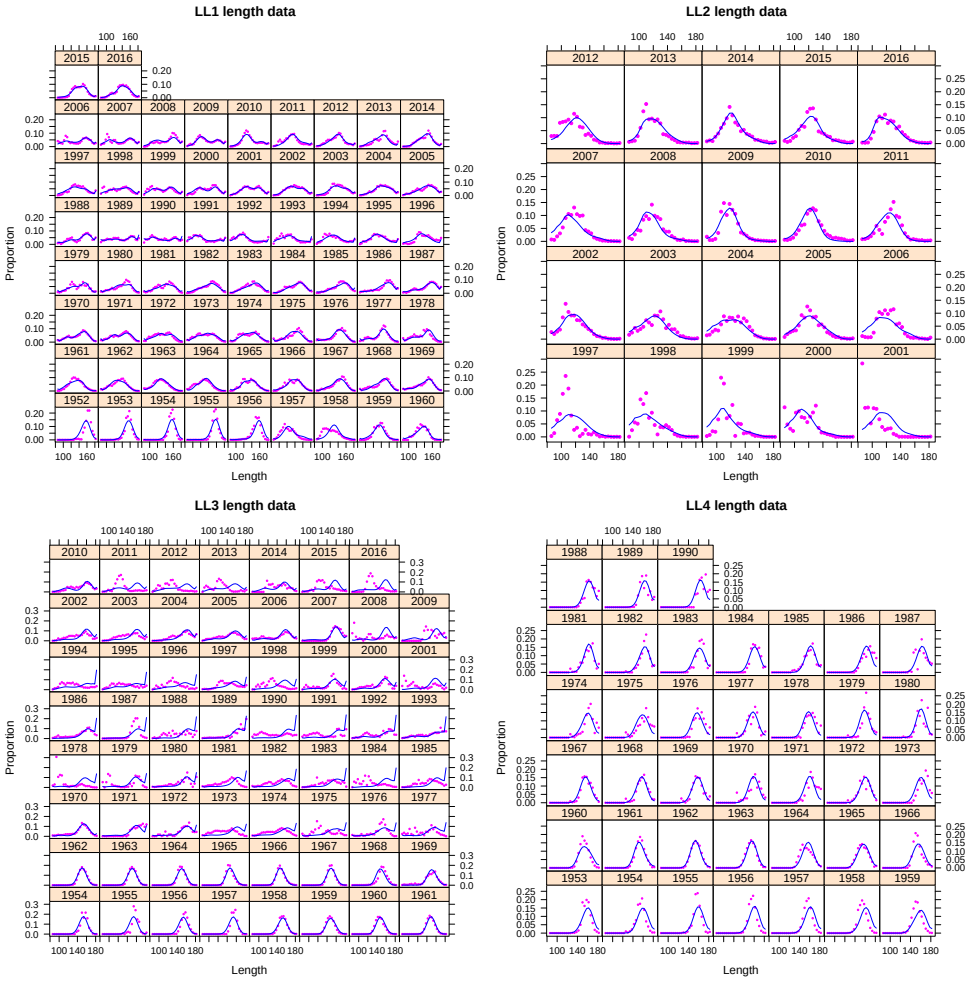

Figure 6.11: *Fits (for the best-fitting grid cell) to the length data for fisheries* LL_{1-4}.

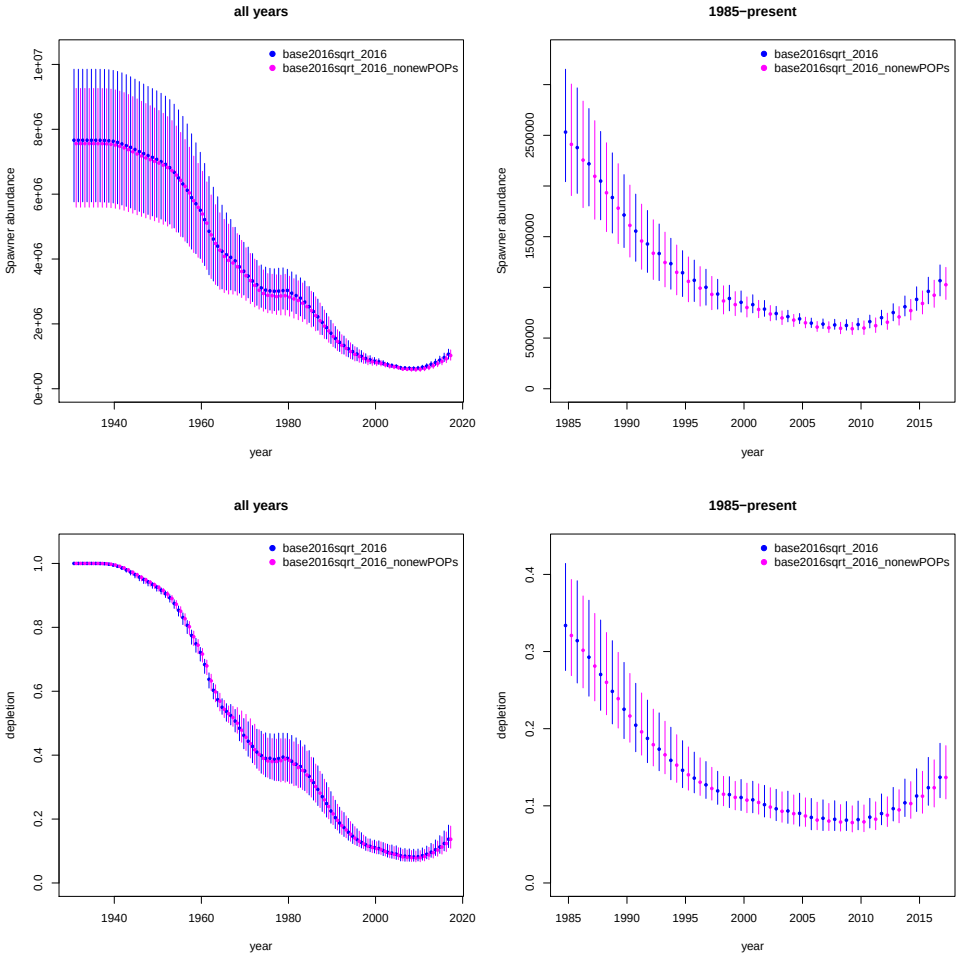

Figure 6.12: *Median and 80% PI summaries for spawner abundance (top) and depletion relative to the unfished state (bottom) for both the full POP data set (**base2016sqrt2016**) and the one with no new POP data (**base2016sqrt2016nonewPOPs**) for all years (left) and from 1985 onwards (right).*

CONTACT US

t 1300 363 400
+61 3 9545 2176
e enquiries@csiro.au
w www.csiro.au

YOUR CSIRO

Australia is founding its future on science and innovation. Its national science agency, CSIRO, is a powerhouse of ideas, technologies and skills for building prosperity, growth, health and sustainability. It serves governments, industries, business and communities across the nation.

FOR FURTHER INFORMATION

CSIRO Oceans and Atmosphere
Rich Hillary
t +61 3 6232 5452
e Rich.Hillary@csiro.au
w